The transition from natural convection to thermomagnetic convection of a magnetic fluid in a non-uniform magnetic field

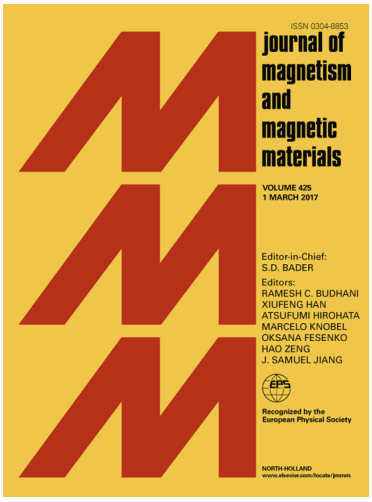

The transition from natural convection to thermomagnetic convection of a magnetic fluid in a non-uniform magnetic field

Peter S.B. Szabo, Wolf-Gerrit Früh

PII: S0304-8853(17)30730-8
DOI: http://dx.doi.org/10.1016/j.jmmm.2017.09.028
Reference: MAGMA 63157

To appear in: *Journal of Magnetism and Magnetic Materials*

Please cite this article as: P.S.B. Szabo, W-G. Früh, The transition from natural convection to thermomagnetic convection of a magnetic fluid in a non-uniform magnetic field, *Journal of Magnetism and Magnetic Materials* (2017), doi: http://dx.doi.org/10.1016/j.jmmm.2017.09.028

The transition from natural convection to thermomagnetic convection of a magnetic fluid in a non-uniform magnetic field

Peter S. B. Szabo[a], Wolf-Gerrit Früh[a]

[a]*School of Engineering and Physical Science, Heriot-Watt University, Riccarton, Edinburgh, EH14 4AS, United Kingdom*

Abstract

Magnetic fluid flow and heat transfer by natural and thermomagnetic convection was studied numerically in a square enclosure. The aim was to investigate the transition from natural convection to thermomagnetic convection by exploring situations where buoyancy and the Kelvin body force would be opposing each other such that the magnetic effects would in some cases be the dominant factor throughout the domain and in other cases only in a part of the fluid. The numerical model coupled the solution of the magnetostatic field equation with the heat and fluid flow equations to simulate the fluid flow under a realistic magnetic field generated by a permanent magnet. The results suggest that the domain of influence over the flow field is largely aligned with the domain of dominance of the respective driving force. The result is that the transition from a single buoyancy-driven convection cell to a single thermomagnetically driven cell is via a two-cell structure and that the local effect on the flow field leads to a global effect on the heat transfer with a minimum of the Nusselt number in the transition region.

Keywords: Natural convection, Thermomagnetic convection, Magnetic fluid, Kelvin body force, Body force ratio

1. Introduction

Magnetic fluids are industrially manufactured colloidal suspensions of magnetic nano-particles with a typical equivalent diameter of about 10 nm. These particles are coated with a surfactant to prevent them from falling out of suspension when dispersed in a carrier fluid. Depending on the application, the carrier fluid could be water, kerosene or a silicone based fluid. Since the first manufactured magnetic fluid in the early to mid-1960s, the magnetic fluids industry has experienced substantial growth as ferrohydrodynamics began to develop [1]. Today, magnetic fluids are used in a range of industrial applications such as in anti-vibration devices or seals, in measurement technology, in medical technology for cancer treatment or targeted drug delivery in the body, and in heat transfer applications such as convection [2]. The electrical conductivity is largely determined by the carrier fluid, leading to the possibility of manufacturing electrically conducting or non-conduction magnetic fluids.

Heat transfer by convection is a key process and well known to transport or remove heat from processes or components by fluid flow in addition to heat conduction. It can be categorised into forced and passive convection. In forced convection, the fluid motion is induced by pumps or fans while in passive convection, changes in some fluid's properties lead to self-induced flow. The most common passive convection is natural or free convection, driven by buoyancy due to temperature-induced density changes. Natural convection in a nanofluid can be modified by a number of processes, such as internal heat generation in electrically conducting fluids or nanofluids with magnetic nanoparticles [3], by a strong variation of the viscosity with temperature [4], or by the shape of the nanoparticles [5], to name but a few. Magnetic fluids exhibit a different type of passive convection, in addition to natural convection, which is not driven by density variations but by changes in the magnetisation of the fluid. This type of convection is called thermomagnetic convection and is described in detail in §1.2. As thermomagnetic convection is not driven by buoyancy, it could be used as a passive cooling mechanism in micro-gravity environments or in situations where the heat source is above the cooling fluid [6]. Before describing thermomagnetic convection, modelling tools used to investigate convection in nanofluids are briefly introduced.

Email address: P.Szabo@hw.ac.uk (Peter S. B. Szabo)

1.1. Modelling approaches of convection in nanofluids

As governing equations for convection of nanofluids are not only the standard thermofluid equations for Newtonian fluids, a choice has to be made whether to simplify the spatio-temporal description or the terms describing the physical interactions. Approaches focussing most on the physical processes are analytical methods which can be applied in systems with a high degree of symmetry, such as a vertical annulus with a uniform magnetic field [7, 8].

Motivated by a number of manufacturing processes, Majeed, Zeeshan and Ellahi [9] investigated the boundary layer flow of an initially stagnant magnetic fluid driven by a stretching sheet while being cooled from the Curie temperature by heat loss through the sheet and subjected to the magnetic field from a dipole just below the sheet. Using the analytic expression for the magnetic field and the linearisation of the temperature sensitivity of the fluid's magnetisation through the pyromagnetic coefficient, they were able to reduce the governing equations to a set of seven ordinary differential equations. This approach proved sufficiently versatile to be adapted to include, for example, chemical reactions [10] or heat radiation [11]. A similar approach was applied equally successfully to analysing natural convection of a conductive nanofluid subjected to a uniform magnetic field [3].

Once the geometry of the system is more complex, one usually has to resort to finite-difference, finite-volume or finite-element methods. For example, the convection of a nanofluid subjected to a constant magnetic field but in an enclosure with an obstacle within could be solved using a Galerkin weighted residual finite element approach [12]. Another option is the Control Volume based Finite Element Method (CVFEM) which exploits the advantages of the two respective approaches, finite volumes and finite elements, for multi-physics problems in complex geometries. Two examples are convection of a nanofluid in an inclined half-annulus [13] or flow of a nanofluid in a porous enclosure with an elliptical outer boundary and an inner block [14]. While these two dealt with complex geometries but simple forcing, the method was also useful for forcing including a magnetic dipole field.

However, all of the above have used constant magnetic fields or magnetic fields prescribed by an analytical dipole field. If the magnetic field itself is not easily written by an explicit equation, finite elements can still be used if the governing magnetic field equations are part of the multi-physics formulation. For non-conducting magnetic fluids subject to a spatially complex but only slowly varying magnetic field, it is sufficient to solve the linear magneto-static equations, either as a separate solution step or as an integrated part of the set of governing equations. Such an approach has in the past been applied [15] and was recently validated against experimental observations [16].

1.2. Thermomagnetic convection

To introduce the essential aspects of thermomagnetic convection, we only focus on the Kelvin body force in this section, which takes the form of $\mu_0 (\mathbf{M} \cdot \nabla) \mathbf{H}$ with the symbols being the magnetic permeabiltiy of free space, the magnetisation of the fluid and the magnetic field [17]. If the temperature sensitivity of the magnetisation is linearised using a so-called pyromagnetic coefficient, K, then, just as volumetric expansion leads to a buoyancy force proportional to the volumetric expansion coefficient, the temperature change and gravity, so does the Kelvin body force lead to a force proportional to the pyromagnetic coefficient, the temperature change and the magnetic field gradient. It has to be noted here that, while the thermomagnetic driving force vanishes at leading order in a uniform magnetic induction field, the temperature sensitivity of the magnetisation also leads to a thermally-induced magnetic field gradient [1].

The effect of a uniform magnetic field gradient on convective instability in magnetic fluids was first discussed in 1970 by Lalas and Carmi [18] and accompanied by Curtis [19] without the presence of gravitational forces. The induced convective flow was based on a magnetisation gradient in a layer of magnetic fluid imposed by a temperature gradient in the presence of a magnetic field gradient and called thermomagnetic convection. A key feature about this is that hotter fluid is less magnetised than cooler fluid. Thus, cooler fluid is more attracted towards higher magnetic field regions than warmer fluid which creates convection when a critical magnetic Rayleigh number is exceeded [1]. For the case of a uniform magentic field gradient parallel to gravity, Blums [17] introduced the concept of an effective Rayleigh number defined as the sum of the standard Rayleigh number and the magnetic Rayleigh number.

The behaviour of different magnetic fluids in the presence of buoyancy and magnetic field forces was investigated experimentally by Sawada et al. [20] and numerically complemented by Snyder et al. [21]. Snyder et al. developed a non-dimensional approach that combined natural and thermomagnetic convection in a single body force term that was expressed as an effective gravity term. While the numerical model was able to exhibit either a natural or a thermomagnetic convection cell, it did not reproduce the transition between these

two cases observed in the experiments in the form of two convective cells. This was suggested to be due to the approximation of the magnetic field from the permanent magnet by a constant magnetic field gradient. Ganguly et al. [22], Mukhopadhyay [23] and Banerjee [24] did consider a spatially varying magnetic field gradient by using the analytical solution of the field for a line dipole instead of a constant field gradient but without including buoyancy. Früh [15] and Szabo [25] considered some cases of thermomagnetic convection in the presence of terrestrial buoyancy and observed that the heat transfer as measured by the Nusselt number can exhibit a transition from natural convection to thermomagnetic convection where the heat flow rate was below that of either natural convection or pure thermomagnetic convection. As this was reminiscent of an observation by Sawada et al., but not captured in the simulation by Snyder et al., this suggested that superposition of buoyancy and magnetic forcing can lead to complex mixed convection but only if the structure of the magnetic forcing includes a realistic spatial structure.

1.3. Aims and Outline

The aim of this study was to develop a better understanding of the consequences of combining natural convection and thermomagnetic convection from non-uniform magnetic field gradients. For the remainder, the flow resulting from combined buoyancy and Kelvin body force will be referred to as 'mixed convection'. This study therefore investigated this mixed convection by re-evaluating the observations of Sawada et al. [20] and extending the earlier study by Snyder et al. [21] using a modelling approach validated against experiments recently [16].

To achieve equivalence to the system by Swada et al., mixed convection in a square cavity driven by a permanent magnet was modelled where the magnetic field was calculated as the Finite-Element solution to the magnetostatic equations. The position of the magnet was chosen to replicate the configuration from Sawada et al., where the magnetic forcing was in the opposite direction to buoyancy (Case 3 in [20, 21]). The remanent magnetisation of the magnet was set to explore in detail the transition from natural convection to a convection cell fully dominated by thermomagnetic convection. The model formulation and computational implementation are introduced in sections 2 and 3, respectively, and the results are presented in §4.

To interpret and quantify the effect of the spatially varying magnetic field gradient on the global flow in section 5, a local force ratio, r, and its average over the fluid volume are introduced. The local force ratio is used to explain the observed flow structures, and the resulting heat transfer is analysed using the Nusselt number as a function of the averaged force ratio.

2. Model formulation

The system investigated was a two-dimensional square cavity filled with an oil-based commercial magnetic fluid with the physical properties summarised in Tab. 1 which was used in a previous study by the authors [16]. The cavity was subjected to thermal forcing by maintaining two opposite walls at a constant temperature whereas all remaining walls were thermally insulated. Figure 1(a) presents the temperature and velocity boundary conditions for the domain.

To investigate the influence of external magnetic fields on the heated cavity, a set of permanent magnets with different remanent magnetisation from 0.1 Tesla to 1.3 Tesla were used. The permanent magnet is $1.2L$ long and has a square pole face with a side length of $0.4L$, where L is the characteristic length scale of the cavity. This was placed with a distance of $0.2L$ above the top centre position of the cavity.

2.1. Governing equations

As the magnetic fluid used here, like the majority of magnetic fluids, has a negligible electrical conductivity, it is here considered as non-conductive [22] and Maxwell's equations in their static form reduce to

$$\nabla \cdot \mathbf{B} = 0 \tag{1}$$

$$\nabla \times \mathbf{H} = 0 \tag{2}$$

where $\mathbf{B}$ is the magnetic induction and $\mathbf{H}$ the magnetic field. The magnetic induction and magnetic field are related by

$$\mathbf{B} = \mu_0 \left(\mathbf{H} + \mathbf{M_M}\right) \tag{3}$$

Table 1: Fluid properties used for the simulations [16].

Property		Value
Carrier Fluid		Mineral oil
Density	$\rho =$	1272 kg/m^3
Thermal diffusivity	$\kappa =$	6.5×10^{-8} m^2/s
Thermal expansion coefficient	$\beta =$	38.5×10^{-5} K^{-1}
Heat capacity	$c_p =$	1554 J/(kg·K)
Dynamic viscosity	$\mu =$	2.614×10^{-2} Pa·s
Kinematic viscosity	$\nu =$	2.056×10^{-5} m^2/s
Volume concentration	$\phi =$	0.1
Magnetic moment	$m =$	$2.93{\times}10^{-25}$ J·m/A
Magnetic bulk saturation	$M_d =$	423 kA/m
Prandtl number	Pr =	316

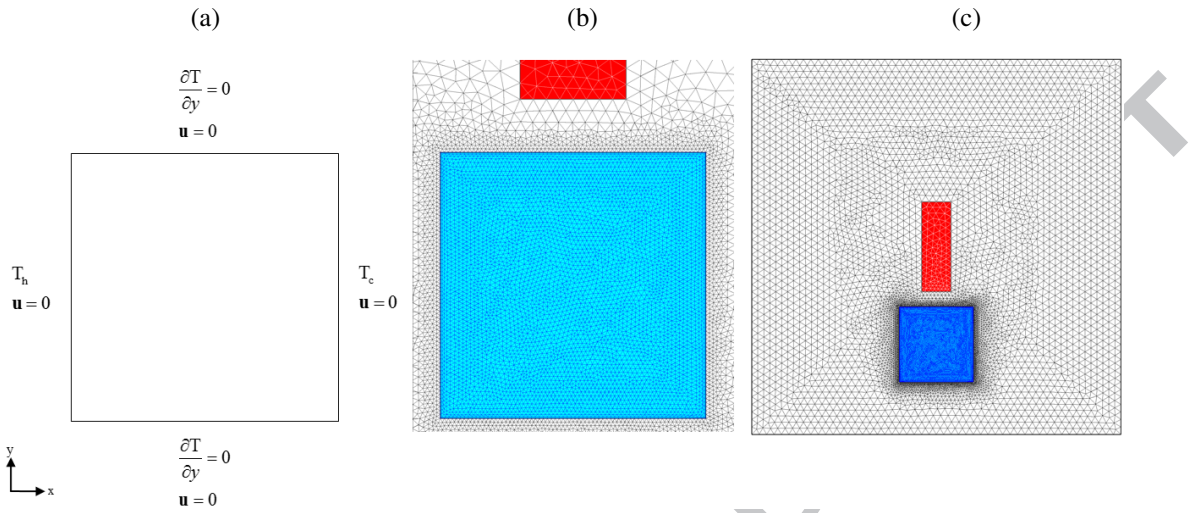

Figure 1: (a) Problem geometry and boundary conditions. (b) Mesh in and near the fluid domain, and (c) the full extended domain used for the solution of the magnetic field equations (blue: fluid domain; red: permanent magnet; white: air)

where μ_0 is the vacuum permeability and has the value $4\pi \times 10^{-7}$ H/m and $\mathbf{M_M}$ the magnetisation of the magnetic material written as $\mathbf{B_r}/\mu_0$ where $\mathbf{B_r}$ is the remanent magnetisation of the permanent magnet.

The assumed magnetic field, $\mathbf{H}$, within the cavity is calculated using the initial Langevin susceptibility written as

$$\chi_{\mathrm{L}} = \frac{nm^2}{3\mu_0 k_B T} \tag{4}$$

where n is the particle number density and equals to $(\mu_0\ \phi M_d/m)$, M_{d} the bulk magnetic of the solid modified by the volume fraction ϕ, m the magnetic moment of the magnetic fluid, k_B the Boltzmann's constant and equals to 1.38×10^{-23}J/K and T the temperature. Following Pshenichnikov et al. [26], the initial Langevin susceptibility may be modified to

$$\chi = \chi_{\mathrm{L}}\,(1 + \chi_{\mathrm{L}}/3) \tag{5}$$

to include inter-particle interactions. Thus, the magnetic field within the fluid domain may be calculated as

$$\mathbf{H} = \frac{\mathbf{B}}{\mu_0\,(1+\chi)} \tag{6}$$

to conform to the magneto-static Maxwell's equations, eq.(1) and eq.(2).

The continuity, momentum and heat equations for a steady incompressible flow are represented as

$$\nabla \cdot \mathbf{u} = 0 \tag{7}$$

$$\rho\,(\mathbf{u}\cdot\nabla)\,\mathbf{u} = -\nabla p + \mu\nabla^2\mathbf{u} + \mathbf{f} \tag{8}$$

$$(\mathbf{u}\cdot\nabla)\,T = \kappa\nabla^2 T \tag{9}$$

where ρ is the density, $\mathbf{u}$ the velocity, p the pressure, μ the dynamic viscosity, κ the thermal diffusivity and the force term $\mathbf{f}$ represents any additional force acting on the fluid. For a thermomagnetic flow in presence of gravity the force term, $\mathbf{f}$, includes buoyancy

$$\mathbf{f_b} = \rho\beta\ \delta T\ \mathbf{g} \tag{10}$$

where $\mathbf{g}$ is the gravitational acceleration and δT the temperature difference to a reference temperature at which the density, ρ, and volumetric expansion coefficient β are defined. It also includes the Kelvin body force

$$\mathbf{f_K} = \mu_0\,(\mathbf{M}\cdot\nabla)\,\mathbf{H} + \frac{\mu_0}{2}\nabla\times(\mathbf{M}\times\mathbf{H}) \tag{11}$$

where $\mathbf{M}$ is the magnetisation of the fluid.

The magnetisation for a mono-dispersed colloidal magnetic fluid is expressed by the superparamagnetisation law [1, 27] through Langevin's function $\mathcal{L}(\zeta) = \coth(\zeta) - 1/\zeta$ written as

$$M_{\mathrm{L}}\,(H,T,\phi) = \phi M_{\mathrm{d}}\ \mathcal{L}(\zeta)\,, \quad \zeta = \frac{mH}{k_{\mathrm{B}}T} \tag{12}$$

where H is the magnitude of the magnetic field. As mentioned when introducing the susceptibility in eq.(5), inter-particle interactions are common in magnetic fluids and eq.(12) is extended to [26]

$$M = \phi M_{\mathrm{d}}\ \mathcal{L}\left(\zeta_p\right), \quad \zeta_{\mathrm{p}} = \frac{m\,(H + M_L/3)}{k_B T}. \tag{13}$$

As fluid velocities are small in natural and thermomagnetic convection and with stationary applied magnetic field, one can assume that the magnetic moment is always aligned with the external magnetic field and the fluid may be considered free from magneto-dissipation so that the last term in eq.(11) may be neglected [22]. Thus, the magnetisation vector, $\mathbf{M}$, may be written as $M\,(\mathbf{H}/H)$. Furthermore, without a temperature gradient the fluid remains stable due to its magnetisation and adiabatic compression, and convection does not occur. However, in the presence of a temperature gradient, the fluid's magnetisation changes such that non-isothermal perturbations of the magnetising field turn to a net driving force from the first term in eq.(11). For moderate temperature differences, this term can be linearised and written as

$$\mathbf{f_K} = \mu_0 K\, \delta T\, |\nabla H| \tag{14}$$

where $K = -(\partial M/\partial T)_{\phi,H}$, is known as the pyromagnetic coefficient.

2.2. Non-dimensional Parameters

In this section, the main non-dimensional parameters are introduced to characterise heat transfer by natural and thermomagnetic convection. A scaling strength of the driving force in natural convection is the Grashof number and presents the ratio of buoyancy to viscous dissipation given by

$$\mathrm{Gr} = \frac{\beta\, \Delta T g L^3}{\nu^2} \tag{15}$$

where ν is the kinematic viscosity and $\Delta T = T_h - T_c$ the temperature difference applied across the system. A similar process to natural convection is found in thermomagnetic convection due to temperature dependencies in the Kelvin body force, eq. (14). Quantifying the ratio of the magnetic forcing through temperature changes in the presence of a magnetic field over diffusion leads to a non-dimensional parameter similar to the Grashof number. This parameter is known as the magnetic Grashof number

$$\mathrm{Gr_m} = \frac{\mu_0 K \Delta T H L^2}{\rho \nu^2}. \tag{16}$$

By introducing further non-dimensional values such as

$$\begin{aligned} u' &= \frac{uL}{\nu}, \quad \nabla' = \nabla L, \quad p' = \frac{pL^2}{\rho\nu^2}, \\ T' &= \frac{T - T_c}{\Delta T}, \quad M' = \frac{M}{\phi M_d}, \quad H' = \frac{\mu_0 H}{B_r} \end{aligned} \tag{17}$$

the computational model equations, both gravitational and magnetic convection, may be considered in non-dimensional form so that eq.(7)-(10) and eq.(14) are given as

$$\nabla' \cdot \mathbf{u}' = 0 \tag{18}$$

$$\begin{aligned} (\mathbf{u}' \cdot \nabla')\, \mathbf{u}' = &- \nabla' p' + \nabla'^2 \mathbf{u}' \\ &+ T' \left[\mathrm{Gr}\, \mathbf{e_g} + \mathrm{Gr_m}\, (\mathbf{M}' \cdot \nabla')\, \mathbf{H}' \right] \end{aligned} \tag{19}$$

$$(\mathbf{u}' \cdot \nabla')\, T' = \mathrm{Pr}\, \nabla'^2 T' \tag{20}$$

where $\mathbf{e_g}$ is the norm vector in the direction of gravity.

The heat transfer is quantified by the Nusselt number, Nu, which is the ratio of the total heat transfer to the conductive heat transfer across a surface where Nu = 1 would indicate a heat transfer by conduction alone and Nu > 1 an enhanced heat transfer by convection. The Nusselt number was calculated by integrating the total heat flux across a cross-section with area A, as

$$\mathrm{Nu} = \frac{L}{\kappa \rho c_p\, \Delta T}\, \frac{1}{A} \int q\, dA \tag{21}$$

where c_p is the heat capacity and q the heat flux across the cross-section, A.

3. Computational methodology and numerical input

The numerical model was calculated with the use of a Finite-Element technique developed [28]. To ensure that the magnetic field of a finite size permanent magnet is correctly solved, the domain was extended by $5L$ in height and width with a zero magnetic scalar potential as the boundary condition. The permanent magnet was placed in the centre of the extended domain as shown in Fig. 1(b), with a remanent magnetisation of $\mathbf{B_r} = (0, B_r)$. The fluid domain was placed according to the specification described in §2 and Fig. 1 in the extended domain.

A triangular mesh was generated with a total of $19,622$ elements where $8,996$ elements were allocated in the fluid domain as is shown in Fig. 1(b) and (c) for each domain, respectively. This mesh was tested

Table 2: Numerical benchmark for natural convection.

Input value Rayleigh no	Result Nusselt no	Vahl Davis Nusselt no	Difference
10^3	1.117	1.116	0.15%
10^4	2.245	2.234	0.50%
10^5	4.526	4.510	0.30%
10^6	8.865	8.798	0.76%

by comparison with the de Vahl Davis benchmark solution [29] for natural convection of a fluid with Prandtl number of $Pr_{air} = 0.71$. The solution was performed by solving the non-dimensional eq.(18)-(20) by using the Rayleigh number, Ra, in Tab. 3 as an input parameter written as $Gr = Ra/Pr_{air}$.

The thermal and velocity boundary conditions presented in Fig. 1 were applied in non-dimensional form so that the temperature was $T' = 1$ for the left heated wall and $T' = 0$ for the right wall. Zero heat flux was applied to the two remaining walls, no-slip velocity conditions to all surfaces, and a zero reference pressure to the top-left corner of the cavity. All configurations were studied with the same initial conditions of a stagnant fluid, a uniform distributed dimensionless temperature, $T' = 0$. As the validation of the model for natural convection obtained sufficiently accurate results, presented in Tab. 2, the fluid used for the validation was replace by the magnetic fluid with the physical properties summarised in Tab. 1.

For this purpose the computational methodology with the magnetic fluid was split into two solution stages. The first stage solved the magnetic field equations eq.(1), eq.(2) and eq.(3) in the full extended domain. Results of the simulated induction field, $\mathbf{B}$, are then used in the second stage to solve the magnetic field, $\mathbf{H}$, inside the magnetic fluid domain using eq.(6) with the fluid temperature, T, defined as

$$T = \Delta T\ T' + T_0 \tag{22}$$

where T_0 is the reference temperature defined as the temperature of the cooled side wall. The resulting non-dimensional magnetic field, $\mathbf{H}'$, is given in Fig. 2. The magnetic field, $\mathbf{H}$, then provided the magnetisation of the fluid, $\mathbf{M}$, and the pyromagnetic coefficient, K, to calculate the Grashof numbers in eq.(15) and eq.(16) which are summarised in Tab. 3. These are then used as input parameters to solve simultaneously the non-dimensional continuity eq.(18), momentum eq.(19) and heat eq.(20). As there is no established convention as to how to specify the magnetic field in the definition for the magnetic Grashof number, eq.(16), the value given in Tab. 3 is the maximum of the local magnetic Grashof number using K and H calculated with the model solutions of the magnetic field and temperature at each node in the fluid domain.

4. Results

The first set of simulations was performed without the magnet, resulting in natural convection, and this is presented in the top row of Fig. 3 with $Gr = 1.1 \times 10^3$. This

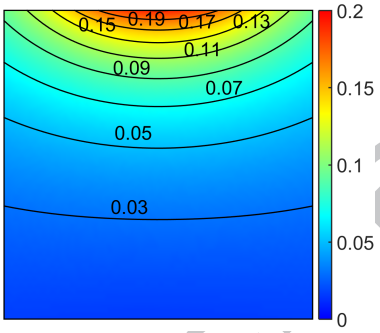

Figure 2: Distribution of the magnitude of the non-dimensional magnetic field, $|\mathbf{H}'|$, within the convection cell.

solution was then used to benchmark the effect of magnetic forces against natural convection for a constant Grashof number. Figure 3(a) with a contour map of the velocity magnitude together with a set of streamlines shows a single, domain-filling convection cell in which the fluid rises adjacent to the heated side wall and descends near the cold side wall with a relatively quiescent fluid in the centre. Figure 3(b) shows the corresponding temperature field as a contour map. This shows the thermal boundary layers at the heated and cooled side walls and relatively flat isotherms in the stably stratified fluid interior.

When the weakest permanent magnet ($\mathbf{B_r} = 0.1$ T) is placed at the top of the cavity, the fluid is magnetised resulting in the additional Kelvin body force, eq. (14). A change in convective flow is observed and is shown in Fig. 3(c) where a second, counter-rotating cell has developed in the part of the fluid closest to the magnet and pushed the original convection cell downwards. The temperature field in Fig. 3(d) shows that there is now a tongue of warm fluid extending from the heated sidewall into the fluid between the two cells, and that cold fluid flows from the cooled sidewall towards the magnet forming a core of fluid that is cooler than the warm tongue below it. This demonstrates that the presence

Table 3: Input parameters for simulation and resulting maximum magnetic Grashof number.

Input values B_r in Tesla	Grashof no Gr	Magnetic Grashof no Gr_m
0.00	1.10×10^3	0
0.10	1.10×10^3	2.32×10^3
0.30	1.10×10^3	7.72×10^3
0.50	1.10×10^3	9.77×10^3
1.00	1.10×10^3	1.04×10^4

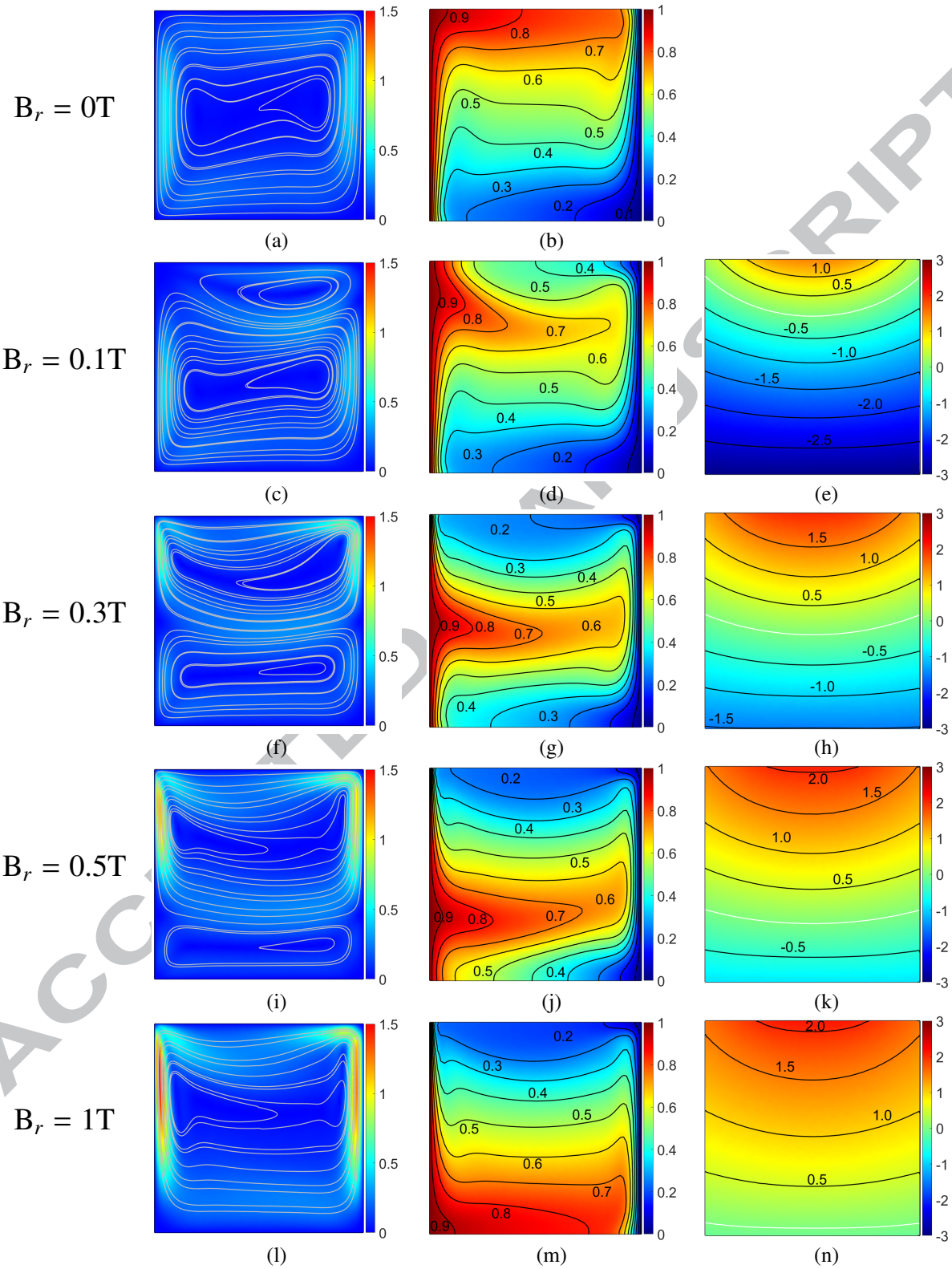

Figure 3: Simulation results for different strength of the permanent magnet. Left column: non-dimensional velocity as colour map with streamlines superimposed; middle column with a colour and contour map of temperature; right column with a colour and contour map of the force ratio, r, where the contour line for $r = 0$ is highlighted in white.

of even a relatively weak magnet creates a thermomagnetically induced convective cell in the top part of the fluid domain while the bottom cell is still dominated by gravitational forces.

To put the observed convection cells and temperature fields into the context of the two driving forces, a measure of their local ratio is defined by

$$r = \log_{10}\left(\frac{\mathrm{Gr_m}\,(\mathbf{M}'\cdot\nabla')\,\mathbf{H}'}{\mathrm{Gr}\;\mathbf{e_g}}\right) \tag{23}$$

and is plotted for all magnetic configurations in the right column of Fig. 3. A value greater than zero indicates that the Kelvin body force is dominant in that part of the fluid domain whereas buoyancy dominates for a value less than zero. For r equal zero highlighted as the white contour line in Fig. 3(e,h,k,n), both body forces are equal. Figure 3(e) shows that the separator between the convection cells is closely aligned with the place in the fluid where the magnitude of buoyancy and Kelvin body force are approximately equal. Placing the second permanent magnet with a higher remanent magnetisation of $\mathbf{B_r} = 0.3$ T at the top of the cavity increases the Kelvin body force throughout the fluid domain. This is reflected in Fig. 3(h) where r increases throughout the entire domain compared to Fig. 3(e). As the higher Kelvin body force within the fluid domain has a stronger impact on the convective flow, the gravitationally dominated flow region decreases, so that the top half of the cavity is now fully dominated by thermomagnetic convection and only the bottom half by natural convection, as can be seen in Fig. 3(f) and (g).

A further increase in Kelvin body force gradually increases thermomagnetic convection overall until the fluid domain is fully dominated by one thermomagnetically induced convective cell which is in this case for a remanent magnetisation of $\mathbf{B_r} = 1$ T, shown in Fig. 3(l) and (m). The disappearance of the gravitationally induced convection cell coincides with the force balance where Kelvin body force exceeds buoyancy everywhere except in a thin layer at the bottom. While the line of $r = 0$ shifts further down with each increase in the magnet's strength, the force ratio near the top boundary does not increase to the same extent. This is due to a weakening of the pyromagentic coefficient as the fluid's magnetisation reaches its saturation level. By $\mathbf{B_r} = 1.3$ T, the force ratio is positive everywhere in the fluid domain.

5. Discussion

The heat transfer across the cavity is quantified by the Nusselt number, Nu, that is plotted versus the remanent magnetisation of each magnet in Fig. 4. The benchmark result of natural convection with Gr= 1.1×10^3 obtains a Nu of 6.84 that decreases when the first magnet is placed at the top of the cavity. The results indicate that the fluid domain which was initially driven by buoyancy is significantly influenced by the thermomagnetically induced Kelvin body force.

The drop in Nusselt number for the first magnetic configuration can be explained by interpreting Fig. 3(c). There, the thermomagnetic convection cell has effectively reduced the available space for the buoyancy convection cell. At the same time, the lateral extent of the thermomagnetic convection cell is limited and it does not reach the left boundary. This is also evident in the temperature profile in Fig. 3(d) where no clear thermal boundary layer is visible near the top of the heated boundary. This means that the convective flow in this upper cell does not contribute effectively to the heat flow from the heated to the cooled side wall. Thus, the net result is a reduction in heat transfer compared to the non-magnetic case. By the next strength of the magnet, the thermomagnetic cell extends fully across the width of the fluid domain and can therefore contribute effectively to the heat transfer. To quantify this effect of the competing body forces on the Nusselt number, an averaged body force ratio may be defined over the entire fluid domain,

$$r_{av} = \frac{1}{A}\int r\, dA. \tag{24}$$

Figure 5 shows how the magnetic Grashof number initially rises with r_{av} but then shows a reversal in $\mathrm{Gr_m}$ followed by a range where it increases rapidly while r_{av} is relatively small. Finally, the magnetic Grashof number seems to approach a saturation value once $r_{av} > 1$. To understand the reversal in the magnetic Grashof number near $r_{av} = 1$, we have to remember, that this $\mathrm{Gr_m}$

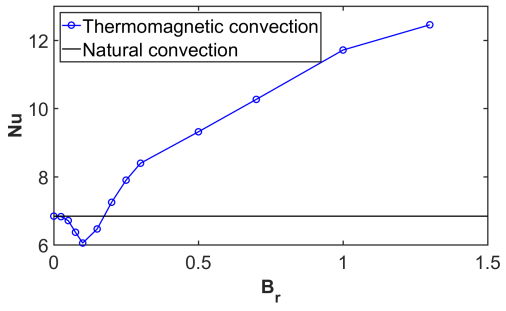

Figure 4: The Nusselt number, Nu, plotted versus the remanent magnetisation, B_r, of each magnet.

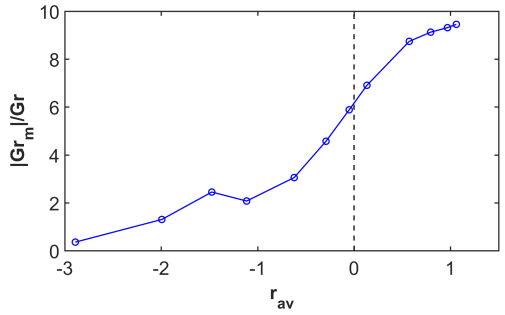

Figure 5: The ratio of Grashof numbers, plotted versus the averaged body force ratio, r_{av}.

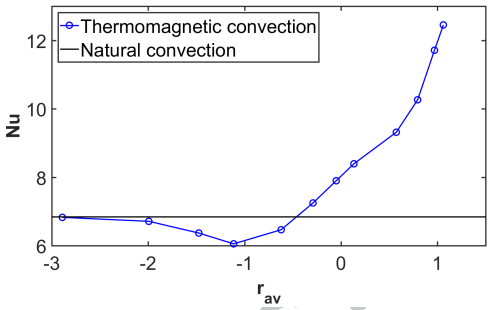

Figure 7: The Nusselt number, Nu, plotted versus the averaged body force ratio, r_{av}.

is not an external non-dimensional parameter but derived from the solution of the system. The temperature fields for the solutions just before and just after the reversal are shown in Fig. 6(a) and (c), respectively. They show that the flow is still a single, gravitationally dominated convection cell before the drop but that a small thermomagnetically driven cell has formed near the upper boundary. Fig. 6(b) and (d) show the corresponding local magnetic Grashof numbers. Initially, the part of the domain closest to the magnet is occupied by warm fluid, transported there by rising under buoyancy from the heated sidewall, once the Kelvin body force is strong

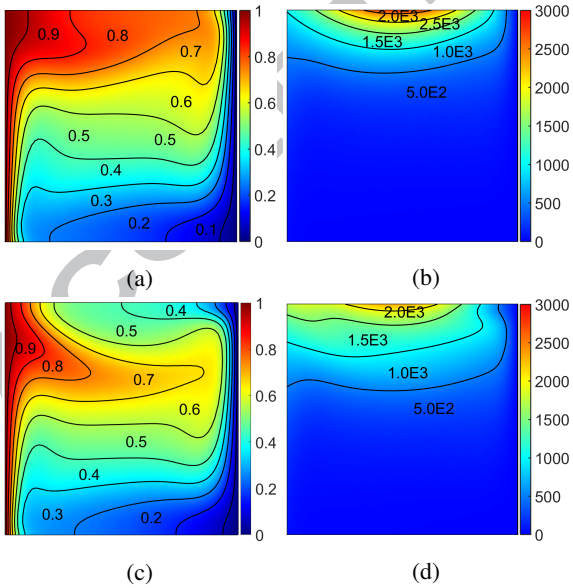

Figure 6: Colour and contour map of temperature left; right column with a colour and contour map of the local magnetic Grashof number; top row for configuration $\mathbf{B_r}$ = 0.075; bottom row for configuration $\mathbf{B_r}$ = 0.1.

enough, it brings cooler fluid to that part, resulting in a change of the local fluid properties, including its temperature and pyromagnetic coefficient. This results in the temporary drop in $\mathrm{Gr_m}$.

Figure 7 shows how the Nusselt number varies against the average body force ratio. From an initial Nu = 6.9, the heat transfer dips initially to Nu = 6.05 at $r_{av} = -1.1$ but then increases rapidly as the thermomagnetic forcing increasingly dominates the flow. At 0.1 T, the Kelvin body force exceeds buoyancy only in the small part of the fluid domain that is closest to the permanent magnet, such that the average force ratio is $r_{av} = -1.1$. In this case, a decrease in Nusselt number to 6.05 is observed, as the magnetically induced thermomagnetic convection is partly suppressing natural convection without being able to contribute constructively to the heat transfer.

By increasing the remanent magnetisation to 0.2 T, the thermomagnetic convection cell reaches fully across to the cooled side wall such that it starts contributing to the overall heat transfer process which is indicated by an increase in r_{av} to -0.3 and an increase in the Nusselt number to 7.2. However, the negative body force ratio states that the overall heat transfer is still primarily driven by buoyancy. If r_{av} reaches a positive value heat transfer is mainly driven by thermomagnetic convection, even if some of the fluid domain is still dominated by natural convection as presented in Fig. 3(h-k). A value of $r_{av} > 1$ indicates that the convection cell is fully dominated by the Kelvin body force and all heat transfer occurs through thermomagnetic convection. Consequently, our study not only captures the previously observed drop in Nusselt number for small externally applied spatially non-uniform magnetic field but also provides clear evidence on the process involved in the transition from gravitationally dominated convec-

tion to thermomagnetically dominated convection.

6. Conclusion

This study has analysed the transition from natural to thermomagnetic convection in a magnetic fluid using the spatially non-uniform magnetic field provided by a permanent magnet. A result of the spatial structure of the magnetic field was that the driving force for thermomagnetic convection was varying substantially over the fluid domain. The cases for this study were chosen to present situations where the Kelvin body force would oppose buoyancy and, with the weakest magnet, be stronger than buoyancy only in a very small region of the fluid to a situation where, with the strongest magnet, it would be stronger than buoyancy almost everywhere.

The results show that the transition is a gradual transition from a natural convection cell to a thermomagnetic cell via mixed convection which is organised into a pair of distinct convection cells: one driven by buoyancy and the other by the Kelvin body force. The dividing line between the two cells is well aligned with the location where the two opposing forces are approximately equal in strength. A relatively sharp transition between flow regimes controlled by either one of two opposing processes, rather than an extended mixed structure, is also found in other convective fluid systems, e.g. [30], but here the transition is determined by the spatial structure and not through a global balance of the forces. As a result, the global effect on the transition can be gradual as the spatial extent of one driving force gradually increases at the expense of the other. This was reflected by the change in the Nusselt number against the average force balance, where the small thermomagnetic cell for the weak magnet reduced the size of the natural convection cell.

Acknowledgements

This work was supported by the Konrad-Adenauer Foundation with a stipend to Peter Szabo.

References

[1] R. E. Rosensweig, Ferrohydrodynamics, Dover Books on Physics, Dover Publications, 1997.

[2] S. Odenbach, Ferrofluids: Magnetically Controllable Fluids and Their Applications, Lecture Notes in Physics, Springer Berlin Heidelberg, 2008.

[3] M. A. A. Hamad, I. Pop, A. I. Md Ismail, Magnetic field effects on free convection flow of a nanofluid past a vertical semi-infinite flat plate, Nonlinear Analysis: Real World Applications 12 (2011) 1338–1346.

[4] M. Sheikholeslami, M. M. Rashidi, T. Hayat, D. D. Ganji, Free convection of magnetic nanofluid considering MFD viscosity effect, J. Mol. Liq. 218 (2016) 393–399.

[5] A. Zeeshan, M. Hassan, R. Ellahi, M. Nawaz, Shape effect of nanosize particles in unsteady mixed convection flow of nanofluid over disk with entropy generation, Proc. Inst. Mech. Eng. Part E J. Process Mech. Eng. (2016).

[6] W.-G. Früh, Heat Transfer Enhancement by Thermomagnetic Convection, Sustainable {(Bio)Chemical} Process Technology (2005) 47–56.

[7] O. Mahian, H. Oztop, I. Pop, S. Mahmud, S. Wongwises, Entropy generation between two vertical cylinders in the presence of MHD flow subjected to constant wall temperature, Int. Commun. Heat Mass Transf. 44 (2013) 87–92.

[8] O. Mahian, I. Pop, A. Z. Sahin, H. F. Oztop, S. Wongwises, Irreversibility analysis of a vertical annulus using TiO2/water nanofluid with MHD flow effects, Int. J. Heat Mass Transf. 64 (2013) 671–679.

[9] A. Majeed, A. Zeeshan, R. Ellahi, Unsteady ferromagnetic liquid flow and heat transfer analysis over a stretching sheet with the effect of dipole and prescribed heat flux, J. Mol. Liq. 223 (2016) 528–533.

[10] A. Majeed, A. Zeeshan, R. Ellahi, Chemical reaction and heat transfer on boundary layer Maxwell Ferro-fluid flow under magnetic dipole with Soret and suction effects, Eng. Sci. Technol. an Int. J. in press (2016).

[11] A. Zeeshan, A. Majeed, R. Ellahi, Effect of magnetic dipole on viscous ferro-fluid past a stretching surface with thermal radiation, J. Mol. Liq. 215 (2016) 549–554.

[12] F. Selimefendigil, H. F. Öztop, Natural convection and entropy generation of nanofluid filled cavity having different shaped obstacles under the influence of magnetic field and internal heat generation, J. Taiwan Inst. Chem. Eng. 56 (2015) 42–56.

[13] M. Sheikholeslami, M. Gorji-Bandpy, D. D. Ganji, S. Soleimani, Effect of a magnetic field on natural convection in an inclined half-annulus enclosure filled with Cu-water nanofluid using CVFEM, Adv. Powder Technol. 24 (2013) 980–991.

[14] M. Sheikholeslami, A. Zeeshan, Analysis of flow and heat transfer in water based nanofluid due to magnetic field in a porous enclosure with constant heat flux using CVFEM, Comput. Methods Appl. Mech. Eng. 320 (2017) 68–81.

[15] W.-G. Früh, Using magnetic fluids to simulate convection in a central force field in the laboratory, Nonlinear Processes in Geophysics 12 (2005) 877–889.

[16] P. S. B. Szabo, M. Beković, W.-G. Früh, Using infrared thermography to investigate thermomagnetic convection under spatial non-uniform magnetic field, International Journal of Thermal Sciences (2017).

[17] E. Blums, Heat and mass transfer phenomena, in: S. Odenbach (Ed.), Ferrofluids: Magnetically Controlled Fluids and their Applications, Springer Verlag, Berlin Heidelberg New York, 2002, pp. 124 – 139.

[18] D. P. Lalas, S. Carmi, Thermoconvective Stability of Ferrofluids, Physics of Fluids 14 (1971) 436–438.

[19] R. A. Curtis, Flows and Wave Propagation in Ferrofluids, Physics of Fluids 14 (1971) 2096–2102.

[20] T. Sawada, H. Kikura, T. Tanahashi, Visualization of wall temperature distribution caused by natural convection in a cubic enclosure, International Journal of Applied Electromagnetics in Materials 4 (1994) 329–335.

[21] S. M. Snyder, T. Cader, B. A. Finlayson, Finite element model of magnetoconvection of a ferrofluid, Journal of Magnetism and Magnetic Materials 262 (2003) 269–279.

[22] R. Ganguly, S. Sen, I. K. Puri, Thermomagnetic convection in a

square enclosure using a line dipole, Physics of Fluids 16 (2004) 2228–2236.

[23] A. Mukhopadhyay, R. Ganguly, S. Sen, I. K. Puri, A scaling analysis to characterize thermomagnetic convection, International Journal of Heat and Mass Transfer 48 (2005) 3485–3492.

[24] S. Banerjee, A. Mukhopadhyay, S. Sen, R. Ganguly, Thermomagnetic Convection in Square and Shallow Enclosures for Electronics Cooling, Numerical Heat Transfer, Part A: Applications 55 (2009) 931–951.

[25] P. S. B. Szabo, W.-G. Früh, Enhanced and reduced natural convection using magnetic fluid in a square cavity, Proceedings in Applied Mathematics and Mechanics 16 (2016) 651–652.

[26] A. F. Pshenichnikov, V. V. Mekhonoshin, Equilibrium magnetization and microstructure of the system of superparamagnetic interacting particles: numerical simulation, Journal of Magnetism and Magnetic Materials 213 (2000) 357–369.

[27] R. E. Rosensweig, Heating magnetic fluid with alternating magnetic field, Journal of Magnetism and Magnetic Materials 252 (2002) 370–374.

[28] COMSOL Multiphysics ®, User's Guide, Version 4.4, 2013.

[29] D. de Vahl Davis, Natural convection of air in a square cavity a bench mark numerical solution, International Journal for Numerical Methods in Fluids 3 (1983) 249–264.

[30] W.-G. Früh, Amplitude vacillation in baroclinic flows, in: T. von Larcher, P. D. Williams (Eds.), Modelling Atmospheric and Oceanic Flow: Insights from laboratory experiments and numerical simulations., AGU Geophysical Monograph Series, Wiley, 2014, pp. 61 – 81.